SANDIA REPORT

SAND2004-5255
Unlimited Release
Printed October 2004

Programmable SAW Development

Robert W. Brocato

Approved for public release; further dissemination unlimited.

Sandia National Laboratories

Programmable SAW Development:
Sandia/NASA Project Final Report

Robert W. Brocato
Sandia National Laboratories
Opto and RF Microsystems
P.O. Box 5800
Albuquerque, NM 87185

Abstract:

This report describes a project to develop both fixed and programmable surface acoustic wave (SAW) correlators for use in a low power space communication network. This work was funded by NASA at Sandia National Laboratories for fiscal years 2004, 2003, and the final part of 2002. The role of Sandia was to develop the SAW correlator component, although additional work pertaining to use of the component in a system and system optimization was also done at Sandia. The potential of SAW correlator-based communication systems, the design and fabrication of SAW correlators, and general system utilization of those correlators are discussed here.

This page is left intentionally blank.

Contents

Nomenclature

AM	-	Amplitude modulated
ASIC	-	Application Specific Integrated Circuit
BPSK	-	Binary Phase Shift Keying
CDMA	-	Code Division Multiple Access
CMOS	-	Complementary metal oxide semiconductor
CSRL	-	Compound Semiconductor Research Laboratory
DC	-	Direct current
DS-CDMA	-	Direct Sequence Code Division Multiple Access
DSSS	-	Direct Sequence Spread Spectrum
FH	-	Frequency Hopping
FPGA	-	Field Programmable Gate Array
FY	-	Fiscal Year
GaAs	-	Gallium Arsenide
GHz	-	Giga Hertz (billion cycles/sec)
HP	-	Hewlett Packard
IC	-	Integrated circuit
IDT	-	Interdigitated Transducer
IF	-	Intermediate Frequency
IL	-	Insertion loss
ISM	-	Instrumentation, Scientific, and Medical frequency band
LC	-	Inductor-capacitor circuit
LDRD	-	Lab Directed Research and Development
LNA	-	Low Noise Amplifier
MATLAB	-	Simulation software available from MathWorks
Mbps	-	Mega bits per second
MHz	-	Mega Hertz (million cycles/sec)
Mm	-	Milli-meters
OOK	-	On-Off keyed modulation
PC	-	Personal Computer
PCB	-	Printed Circuit Board
PN	-	Pseudo Noise
POP	-	Peak-Off-Peak ratio
PSL	-	Peak-to-SideLobe ratio (same as POP)
PSPICE	-	PC version of SPICE available commercially
RF	-	Radio Frequency
RFID	-	Radio Frequency Identification
RMS	-	Root Mean Square
SAW	-	Surface Acoustic Wave
SNR	-	Signal to Noise Ratio
SPICE	-	Simulation Program with Integrated Circuit Emphasis
SS	-	Spread Spectrum
UWB	-	Ultra-Wide Band

Executive Summary

This report describes the development of a fundamentally new kind of radio, based on a new kind of architecture. The initial application for this new type of radio is space-based communications, but this can easily be extended to a wide range of other applications. Potential barriers to adoption of new technology are high, and radio design is no exception. The desired goal is to build a very small, very low power commercial radio receiver by combining a number of physically large, powered components into a single, passive component, the SAW correlator. Commercial wireless product developers are currently focused on techniques that are fundamentally limited in their ability to reduce size and power. IEEE standard 802.11x variant radios are becoming commonplace, but are still more than an order of magnitude greater in both size and power consumption than where they need to be for the next generation of micro-wireless communications.

The approach of this work represents a fundamental departure from the conventional approach taken to construct a very small radio receiver. Conventional radio systems go through a number of subsystems to convert data into the transmitted radio signal and vice-versa. Through sheer force of engineering effort, and with the expenditure of billions of dollars, these systems have been refined to the high level of sophistication present today. The size and power consumption of these systems have decreased dramatically in the last 20 years, but without fundamental changes in approach. As a result, it is increasingly difficult to obtain further decreases in size or power consumption using these convention approaches.

The approach taken in this work is to combine the functions of many, sophisticated microwave and digital signal processing sub-systems into a single component, the SAW correlator. This single component, operating in transmission mode, accepts baseband data and passively transforms it into a complex, broadband, bi-phase coded microwave signal. The SAW correlator can also be operated in a reverse manner to demodulate the same complex, broadband bi-phase coded microwave waveform into baseband data. The SAW correlator operates without requiring any DC power, although support circuitry may require some DC power. When used in conjunction with optimized support circuitry, it holds the potential to deliver at least 10x smaller and lower powered wireless receivers.

The idea of using SAW correlators as the basis for radio communications is not new. Attempts to use a SAW correlator as a matched filter for radio communications date back to at least 1974 [1]. Early SAW correlator-based systems operated as conventional heterodyne-type radios. The correlator was used as a signal-processing element at IF. Basic spread spectrum systems using SAW correlators were reported in 1980 at HP Laboratories [2]. These early systems were hampered by an inability to fabricate devices that operate directly at the transmission frequency. As a result, they still needed the same large, power consuming mixers and oscillators that were required by conventional methods [3]. In addition, these systems were hampered by two other fundamental problems. First, the early makers of correlator lacked the lithographic accuracy, manufacturing controls, and process stability needed to reliably produce large quantities of SAW correlators. Second, each correlator code needed for each radio had to be separately produced as a distinct and unique component. That is, the correlators lacked easy programmability. The early techniques showed limited promise for reducing power consumption and size, and they did not lend themselves to the mass production techniques needed for commercial acceptance.

In the course of our development work on the correlators, we used modern lithographic and micro-system fabrication techniques that enabled us to overcome all of the limitations of the early systems. The use of electron beam lithography enabled the fabrication of fixed SAW correlators and filters that operate directly in the microwave band centered at 2.43 GHz; this band was selected as a desirable communication frequency for NASA applications. Fixed correlators that operate at 62 MHz, 183 MHz, 915 MHz, 2.7 GHz, 4.6 GHz, and 5.7 GHz were also successfully fabricated and tested. Multiple fabrication runs demonstrated the capability to reliably fabricate repeatable results with sufficient

frequency stability for use in NASA's application. Fabrication was conducted on both temperature stable (ST-X cut quartz) and low loss (Y-Z lithium niobate) materials. Adequate software modeling of SAW correlators was found to be unavailable commercially, and so was developed in house. MATLAB, MathCAD, and SPICE-based models were developed for progressively more sophisticated simulations, in the order given. Fabrication, testing, and packaging of fixed code SAW correlators were demonstrated. Three different variants of electrically programmable surface acoustic wave (PSAW) correlators were developed, tested, and demonstrated. These PSAW correlators operate at 300 MHz, 915 MHz, and 183 MHz. The successful demonstration of the PSAW overcomes the manufacturing limitation that required a separate SAW correlator to be fabricated for each coded receiver.

At the system level, a basic communication link utilizing SAW correlators operating at 2.43 GHz was developed and demonstrated. The system used OOK communication with fixed SAW correlators for direct RF-to-baseband conversion in both the transmitter and receiver. The purpose of the system was to demonstrate the possibilities of communication using SAW correlators. Low power communications were demonstrated in a high multi-path environment over 10m links.

The most significant product of the project is the development of the PSAW. As was mentioned, in all early systems, a different correlator had to be fabricated for each transmitter/ receiver pair. If a receiver needed to listen to several transmitters, then it needed to have a separate correlator for each device that it needed to listen to. With the PSAW, a single SAW device is built for all transmitters and receivers in a system. The radio then electronically adjusts its correlator for the transmitter that it is to listen to, or the receiver that it is to talk to.

Although the work described in this report is seminal, it will require significant follow-on engineering efforts to produce large quantities of field-ready systems. We have reported the development of the PSAW in the technical literature [4]. We have also described the possibilities for using fixed SAW correlators for ultra-wideband communications [5]. Additionally, we are not the only group interested in pursuing this technology. High frequency correlators have been developed for a 2.4GHz spread spectrum modem [6], and more recently, a multi-carrier spread spectrum modem operating at 2.4GHz was demonstrated [7]. Recent work with SAW filters indicates the feasibility of extending these operating frequencies to 10GHz [8]. The intent of this report is to demonstrate the technology, its manufacturability, and its ultimate possibilities.

Technical Background
This new approach to radio receiver design is based on a SAW correlator. In its simplest form, a SAW device appears as two comb-like metal structures deposited on a piezoelectric crystal surface (figure 1).
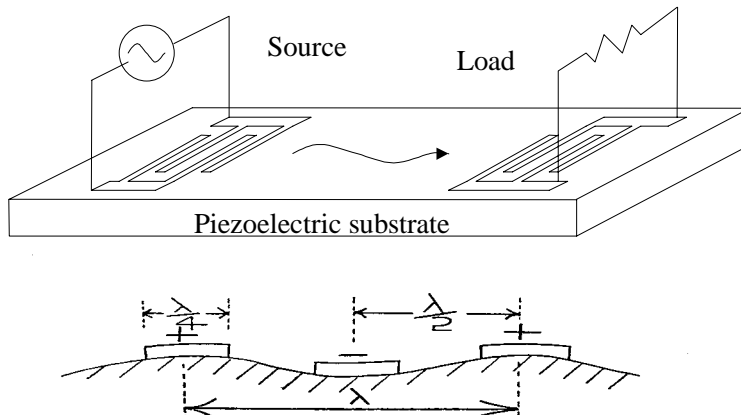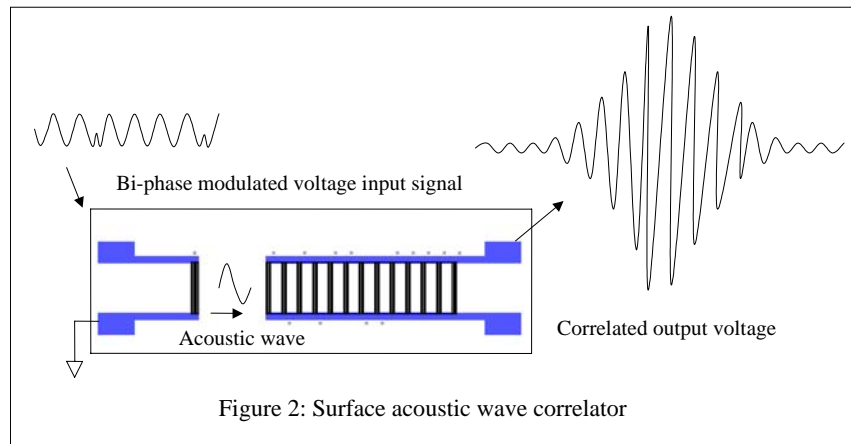

Figure 1: Surface Acoustic Wave Device

The first comb-like structure serves as a transducer to convert long wavelength radio waves to very short wavelength acoustic waves. For instance, a 3 GHz radio wave propagating in free space has a wavelength of 10cm, while a 3 GHz acoustic wave propagating in lithium niobate, a suitable piezoelectric material, has a wavelength of 0.000116 cm. The SAW takes advantage of this wavelength compression to perform signal processing on radio waves within the physical space constraint of a small chip. The second comb-like structure in the SAW serves both as signal processing device and as a transducer to convert the acoustic waves back into an electromagnetic signal.

Although SAW devices may not be widely understood, they are very widely used and have been around for over 35 years. SAW filters are commonly used in many consumer electronic devices. A typical cellular phone contains several SAW filters. The worldwide production of SAW devices was estimated to be nearly 1 billion devices in 1997 [9]. SAW filters also have a long history of production and use at Sandia Labs. Sandia uses SAW filters for communication applications and a wide variety of sensor related products. For example, the MicroChemLab is a Sandia chemical sensor-on-a-chip that uses SAWs to detect a range of different chemicals. In contrast to SAW filters, SAW correlators are not widely used in industry, although research into these devices has been conducted for over 30 years.

Bi-phase modulated voltage input signal

Acoustic wave

Correlated output voltage

Figure 2: Surface acoustic wave correlator

A SAW correlator is a two transducer piezoelectric device used to provide a matched filter output (figure 2). The filter, in the case used here, matches to a BPSK phase modulated signal, rather than the usual sine wave. That is, the incoming radio wave has 180 degree phase transitions in its sinusoidal waveform, modulated in a coded pattern. A transducer, or IDT, in the front end of the SAW correlator converts the electromagnetic wave to a surface acoustic wave. SAW correlators use this electromagnetic to acoustic wavelength compression to perform bi-phase coded signal processing on the resulting acoustic wave. The correlator first has a transducer to convert radio waves into acoustic waves at a selected center frequency and with a selected bandwidth. The correlator then has a phase coded receiver transducer to convert the correctly phase coded acoustic wave into an RF modulated electrical pulse. Envelope detection of the modulated pulse yields a base-band electrical pulse. This pulse can be used for low data rate communications or to turn on a higher-power consumption, higher-data rate receiver. The correct correlation coded signal is essentially a long multi-bit "key". The correlator output signals the correct "key" by outputting a voltage spike. If an incorrect code is given, the correlator output appears similar to broadband, low-level noise.

The correlators used in this work make use solely of BPSK signals. It is possible to use correlators with other forms of encoding. However, phase coding offers the best SNR, and BPSK is the simplest form of phase coding. The correlator can provide considerable process gain by converting the long input BPSK signal with a matched pattern into a short RF modulated pulse with an envelope at the baseband frequency. The baseband envelope pulse is then recovered using a microwave detector diode operating

optimally in its square law region. A high frequency correlator can be used without IF stages by directly converting the input coded RF signal into an output baseband pulse. Figure 2 shows this basic receiver approach with the SAW correlator's output section divided into the equal phase-coded sections referred to as "chips". The modulated output pulse of such a device operating at 2.4GHz is shown in figure 3. The number of chips in the correlator determines the code length of the device. This analog conversion approach rejects multi-path and other spurious signals to the same degree as comparable DSSS systems. The correlator can be operated in forward or reversed mode to produce low power, low component count receivers and transmitters.

A significant drawback to using this approach is the limited code length that can be achieved with conventional SAW correlators. The SAW correlator output transducer converts acoustic energy to electrical energy, typically being electrically terminated in some low impedance, such as 50Ω, to enable high frequency operation. Each chip section of the output transducer converts a portion of the acoustic wave that passes under it into electrical power in the real part of the output impedance. By the time the acoustic wave has passed under about 30 chip-sections of the output transducer, its amplitude has decayed so significantly, that there is little signal left with which to do further correlations. Figure 4 shows the output response of a 2.43GHz, 31 chip long SAW correlator after it has been excited with a burst of RF at the center frequency of the device and with a number of cycles equal to the number of cycles in one chip. This excitation waveform essentially forces the correlator to spit out its RF modulated code. The noteworthy aspect of this figure is the rapid decay in amplitude of the output waveform from the first chips to the last. Each successive wave in the plot is a single, RF-modulated chip. The amplitudes of these successive waves decrease about 95% from the first chip to the last. This rapid decay is a direct result of operating the high speed SAW by having it drive a low electrical impedance. This decay effect was much less significant in low frequency, high impedance devices [10]. This decay in correlator response has the same effect when operating as a receiver and severely limits the useful code length of the correlator for high-speed devices. Maximum code length for a 50Ω correlator was found to be about 31 chips, due to this effect.
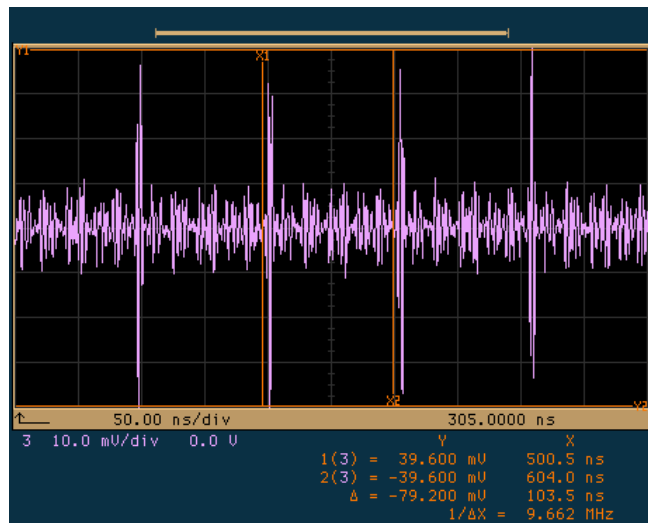

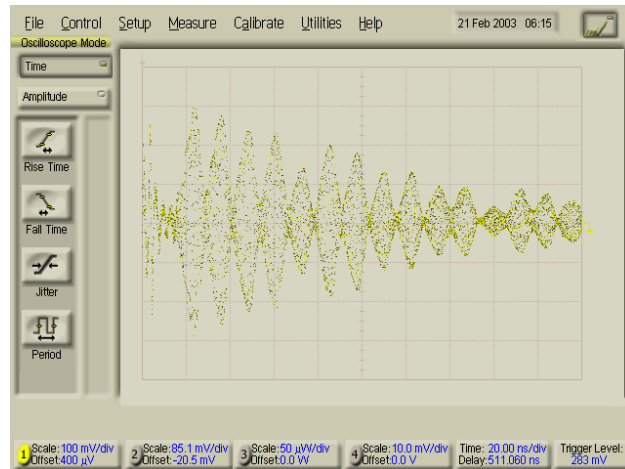Figure 3: SAW correlator output at 2.43GHz.

Figure 4: SAW correlator output in reverse mode.

SAW Correlator Modeling

Software for modeling SAW correlators is not available to be purchased commercially. A few basic software packages exist for modeling SAW filters and resonators, but these programs possess very limited capabilities and do not have the ability to model correlators. To aid the correlator design process an effort to develop MATLAB models was undertaken and completed by means of a contract with the University of New Mexico. The MATLAB simulation models include SAW filter and basic SAW correlator functions. This software has been made available without charge to the general public as a MATLAB library on a public domain Internet site.

A basic mathematical model of the SAW correlator was constructed in MATLAB. Figure 5 is the simulated output of a SAW correlator with a 10% input bandwidth and a code length of 127. The spread spectrum code implemented in the correlator is a type of code referred to as a maximal length sequence (i.e. m-sequence code). The MATLAB simulation software is based on the delta-function model. The delta-function model treats each SAW transducer element as a delta function in a finite series of delay elements. It is really a representation of an ideal transversal filter. This model treats the correlator as an ideal mathematical element rather than a physical element. Since it is not a physics-based model, it simulates quickly, but does not include sufficient information detail for correlator design. It does not include the effects of energy removal and wave modification discussed in the previous section. These can be considered to be second order effects, but in the design of a correlator, they are of significant concern. For instance, if one would like to optimize the peak-to-sidelobe (PSL) ratio of the correlator either through design of the correlator or through code selection, the MATLAB model is inadequate. This model will indicate general advantages and disadvantages of different codes, but it will not faithfully reproduce actual SAW correlator output waveforms. This is because the delta function simulation does not take into consideration the energy lost to the load and the waves re-transmitted when a wave impinges on a given finger-pair of the correlator. The delta function model essentially assumes that each finger-pair of the correlator represents infinite electrical impedance, and this assumption becomes increasingly inaccurate the higher one goes in frequency. Since high frequency electronics are typically designed to be matched to 50Ω, the correlators are also designed to be matched to this impedance. This 50Ω load removes energy as the wave passes under each finger-pair of the SAW, thus lowering the wave amplitude as the wave energy is intercepted by the output section of the correlator.
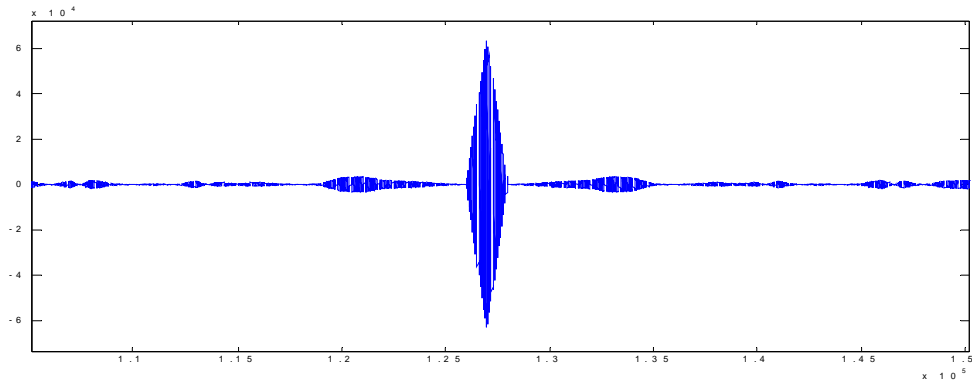
11

Figure 5: MATLAB delta function simulator output

The MATLAB-based simulation software runs quickly on a personal computer, and enables the rapid, but high-level investigation of different correlator designs. A second modeling effort was undertaken at Sandia to develop a model for SAW correlators that includes material properties, electrical parasitics, and physics-based device effects. This modeling effort was completed in SPICE. The simulation software uses SPICE (either PSPICE or ChileSPICE) as a solver engine on an electrical model of the SAW device. The SAW model used is a crossed-field model derived from the Mason equivalent circuit [11]. It models each device as a three port admittance network and makes use of transmission line delay elements in SPICE to simulate the acoustic effects of the material. Two of the ports are for the traveling acoustic wave, and one of the ports is for the electrical interaction of the fingers with the acoustic wave. The resulting model looks like a long string of three port transmission-line segments (figure 6). Each individual chip of the SAW is modeled as a single element. A 15-chip SAW correlator receiver looks like a long string of sequentially connected elements (figure 7). This sequential string is provides a good simulation of the actual sequential connection of the SAW receiver elements.

Figure 6: Mason-equivalent model of a single SAW finger-pair
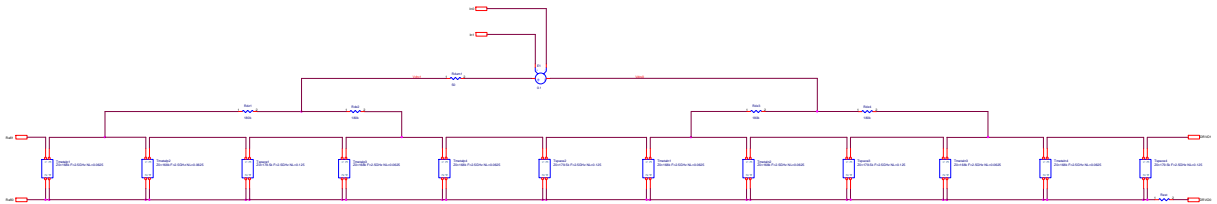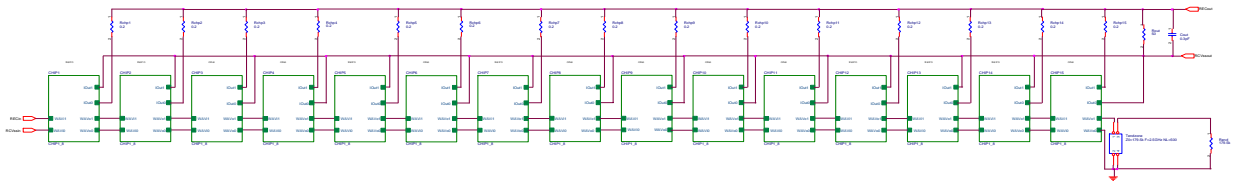

Figure 7: Hierarchical model of a 15-chip SAW correlator receiver

The SPICE simulation is also capable of including various electrical parasitic components that unavoidably occur in the fabrication and operation of a programmable correlator. The model includes acoustic end reflection and bulk wave effects. It has proven useful for evaluating the relative advantages

12

of SAW physical layout variations (figure 8). In this figure, three successive code sequences were sent. At first, the PSL ratio is low as the correlator is essentially being asynchronously filled. Sidelobe variations are high, as even the mathematical model will predict. When the second code sequence begins to fill the correlator, immediately after the first correlation peak but before wave reflections have much impact, the PSL ratio is very high. This is synchronous filling of the correlator, and the high performance PSL results are the same as the mathematical model predicts. Shortly after the second correlation peak, the wave reflections have a significant impact and the model represents what is routinely seen with actual physical devices. That is, the synchronously filled physical model of the correlator has an output PSL ratio that is about the same as an ideal mathematical model will predict for an asynchronously filled correlator. These simulations are very computationally intensive, so some simulations were run on one of Sandia's supercomputers, Discovery. The non-parallel nature of the simulations does not lend itself to a significant speed improvement from running on a large, parallel machine. PC simulations were found to be nearly as fast and much more convenient. The simulation shown in figure 8 required about 15 hours of computer run-time.
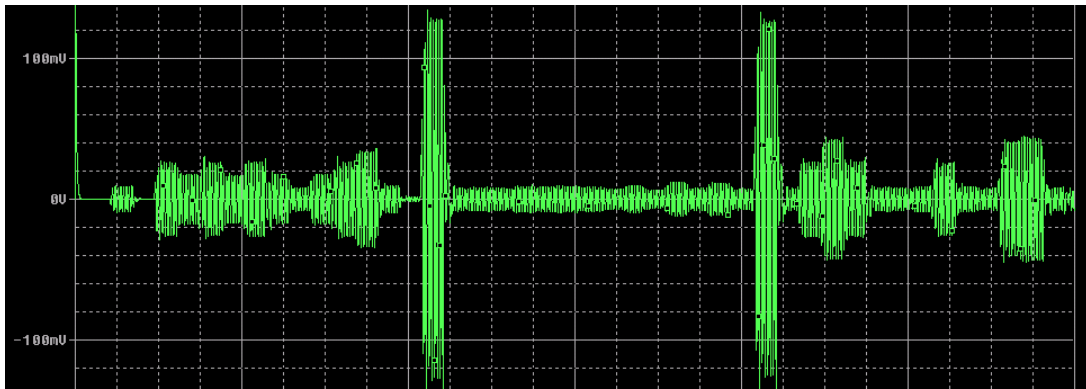

Figure 8: SPICE simulation output of programmable SAW correlator including electrical parasitics and end reflection effects.
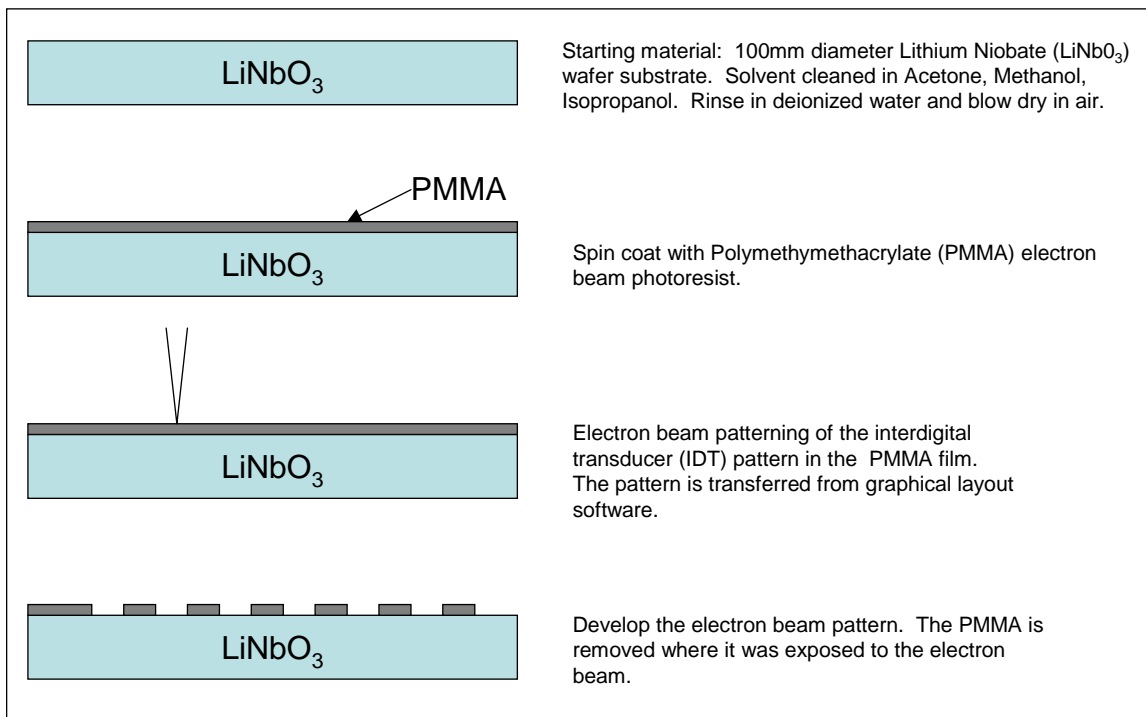
Fixed SAW Correlator Fabrication
Since it is necessary to be able to successfully fabricate high performance, fixed SAW correlators before an adequate programmable device can be made, a great deal of our available effort went into optimizing fabrication of fixed SAW correlators. The fabrication of the SAW correlators on lithium niobate and quartz makes use of both optical and e-beam lithographic technologies. A combination of SAW filters, for process diagnosis, and fixed SAW correlators, as usable communication devices, are made on each fabrication mask set. The SAW filters and correlator structures are generally fabricated using industry-standard processing methods. The SAW devices are produced using a two-step lithography process wherein the fine-line IDTs are patterned in a first step, followed by a metal bond pad layer that is patterned in a second step. Different types of metals are used on the two different layers. The IDT layer metal is 500Å of aluminum. This metal layer is kept thin to minimize acoustic reflections from the IDTs. The second metal layer consisting of 5000Å of gold is added to provide mechanical bond strength and good conductivity of RF signals from bond pads to the IDTs. Contact optical photolithography patterning methods are used wherever possible. Electron beam lithography methods must be used for finger patterning for device frequencies above approximately 800 MHz. In those cases, an electron beam lithography step is used to fabricate the IDTs, followed by an optical lithography step to define the bond pad layer. An alignment structure is always included in the layout to correctly align the layers during processing.
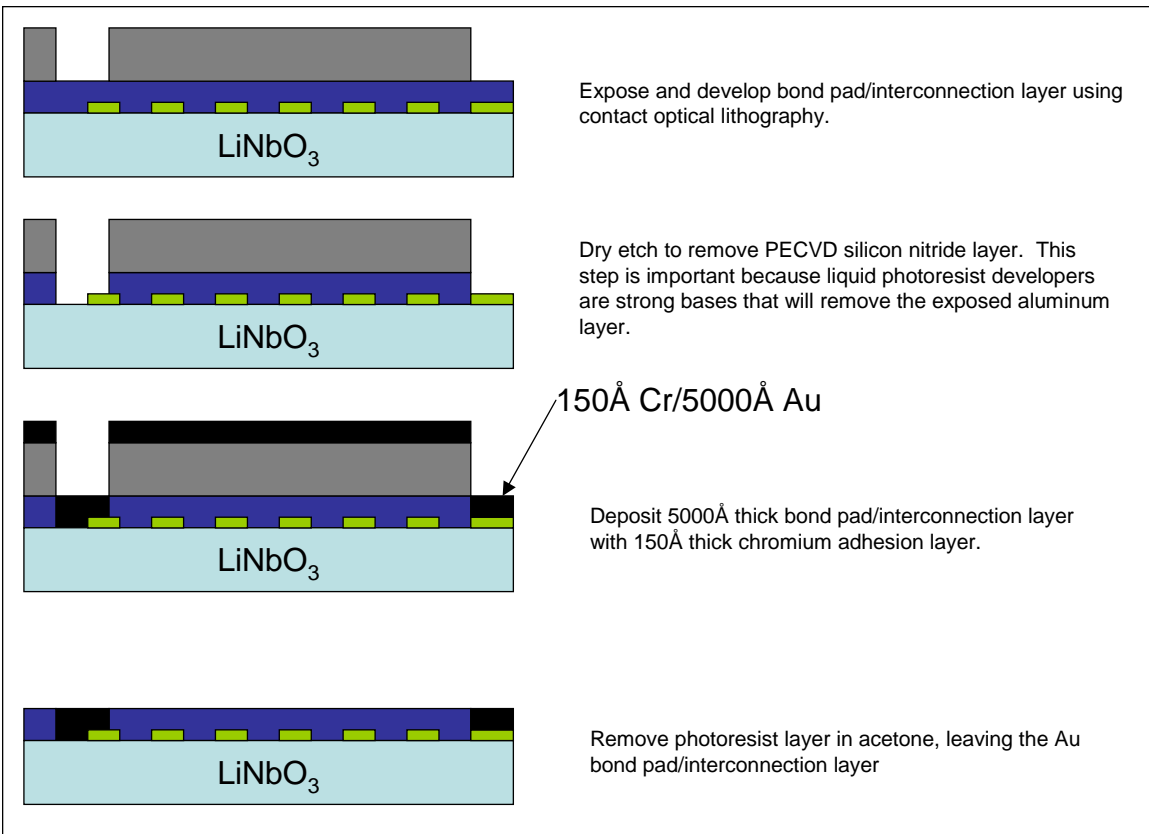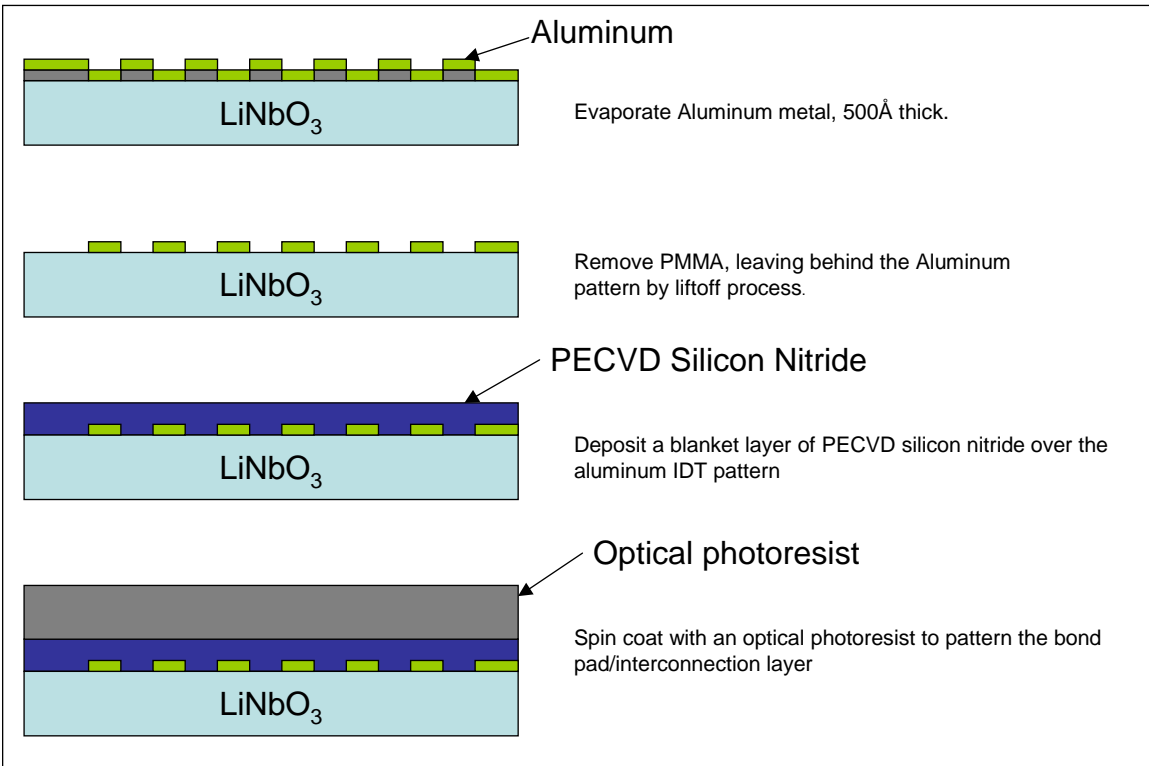
The starting substrate material is a 100 mm diameter, circular, lithium niobate wafer. There are different crystal orientations available, and each orientation will give different characteristics such as velocity,
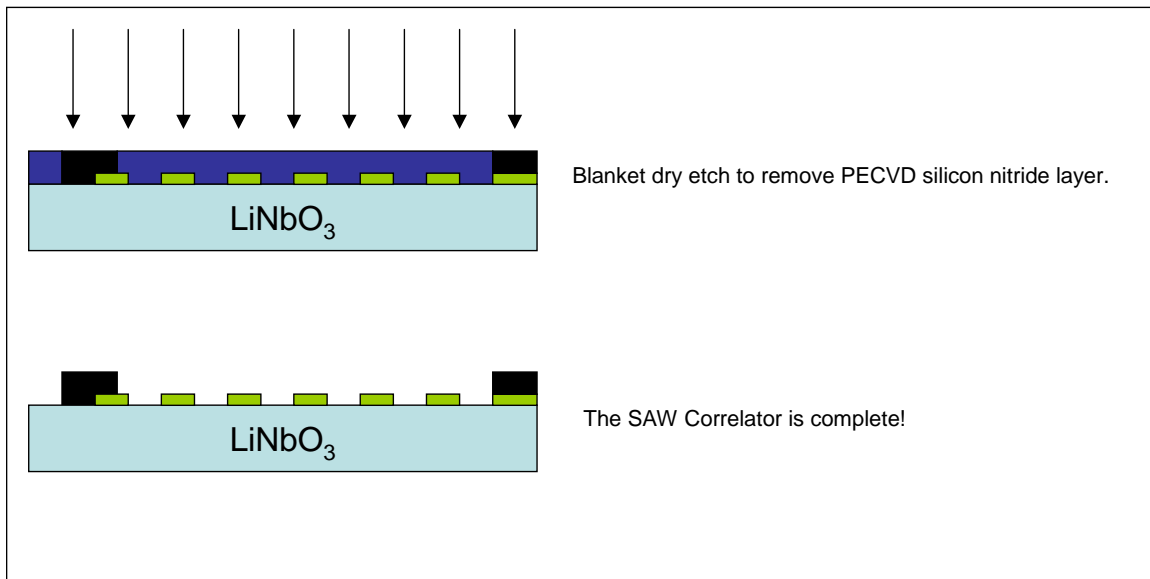
temperature coefficient, etc. Most of the SAW devices fabricated for this work use Y-Z cut lithium niobate with an acoustic velocity of 3488 m/s. The wafers used are only flat to electronic-grade tolerance, not optical-grade tolerance. This will limit the performance of the correlators at frequencies above 4GHz, as the less even surface will contribute to wave dispersion. The wafers have very few particles and are very clean directly from the manufacturer, but an organic solvent rinse is used to remove residues that may accumulate during shipping. Many standard pre-cleaning methods can etch lithium niobate, so the organic solvent must be chosen carefully. The IDT layer is patterned on the substrate using a standard liftoff process. That is, the aluminum for the IDT layer is deposited on top of patterned photoresist, which is then selectively removed, leaving a patterned aluminum IDT in contact with the substrate. Following the IDT layer, the wafers undergo both solvent and oxygen plasma cleaning processes to remove organic residues.

The metal bond pad layer is patterned on the wafer after the IDT processing is complete. The lithography of the metal bond pad layer is also usually a routine liftoff process. However, most photoresist developers etch the aluminum in the IDT layer. So, the fine aluminum fingers must be protected. Also, as the developer removes exposed photoresist, it begins to etch the bus-bars. A simple multi-step process has been used to alleviate this difficulty. First, a blanket layer of silicon nitride is deposited over the entire wafer, and metal2 (gold- on-chromium) for the bond pads is patterned over the top of the silicon nitride. The open areas of the gold are then processed using dry plasma etch through the silicon nitride to expose the aluminum IDT metal. The plasma silicon nitride etch process does not etch the aluminum bus-bars as the liquid photoresist does, and the bus-bars remain exposed. The 5000Å thick gold layer is then deposited with an underlying 150Å thick chromium adhesion layer. This leaves the bond pad metal fully patterned. Finally, following liftoff of the gold layer, a blanket-etch of the silicon nitride exposes the entire wafer. At that point, the process is complete and the SAW devices are ready for testing.

All of the processing steps used to make SAW devices at Sandia are shown in the accompanying charts:

Starting material: 100mm diameter Lithium Niobate ($LiNbO_3$) wafer substrate. Solvent cleaned in Acetone, Methanol, Isopropanol. Rinse in deionized water and blow dry in air.

Spin coat with Polymethymethacrylate (PMMA) electron beam photoresist.

Electron beam patterning of the interdigital transducer (IDT) pattern in the PMMA film. The pattern is transferred from graphical layout software.

Develop the electron beam pattern. The PMMA is removed where it was exposed to the electron beam.

Aluminum

LiNbO$_3$

Evaporate Aluminum metal, 500Å thick.

LiNbO$_3$

Remove PMMA, leaving behind the Aluminum pattern by liftoff process.

PECVD Silicon Nitride

LiNbO$_3$

Deposit a blanket layer of PECVD silicon nitride over the aluminum IDT pattern

Optical photoresist

LiNbO$_3$

Spin coat with an optical photoresist to pattern the bond pad/interconnection layer

LiNbO$_3$

Expose and develop bond pad/interconnection layer using contact optical lithography.

LiNbO$_3$

Dry etch to remove PECVD silicon nitride layer. This step is important because liquid photoresist developers are strong bases that will remove the exposed aluminum layer.

150Å Cr/5000Å Au

LiNbO$_3$

Deposit 5000Å thick bond pad/interconnection layer with 150Å thick chromium adhesion layer.

LiNbO$_3$

Remove photoresist layer in acetone, leaving the Au bond pad/interconnection layer

Blanket dry etch to remove PECVD silicon nitride layer.

The SAW Correlator is complete!

Fixed SAW Correlator Results
Technical issues involving the fixed SAW correlators fall into three main areas of discussion: impedance matching, temperature effects, and electrical performance. Any improvements to the fixed SAWs and any applications that make use of them in a system should consider the lessons learned from these development areas.

Impedance Matching
A crucial issue to be resolved in the development of a complete spread spectrum system using SAW correlators is impedance matching. Due to the physical nature of the SAW transducer elements, the electrical impedance seen looking into the SAW correlator is not a good match for any practical antenna. This arises from the physical structure of a SAW correlator. To preserve signal phase transitions, the input IDT for a SAW correlator must not be wider in quantity of finger-pairs than the number of cycles between code phase transitions in the signal. The width of the correlator input IDT determines the input bandwidth of the correlator in an inverse relationship. The number of code phase transitions in the correlator receiver IDT determines the bandwidth of the received signal, also in an inverse relationship. If the input IDT were to be wider than the number of cycles between phase transitions, then the input bandwidth would be narrower than the signal bandwidth. This means that a SAW correlator with 127 code phase transitions will have an input IDT that is less than or equal to $1/127^{th}$ of the size of the receiver section. Such a device is inherently unbalanced from an impedance matching perspective. If the output section is adjusted in width or number of finger-pairs to appear close to 50Ω at the center frequency of the device, then the input will appear as a small capacitor with a very small series resistance, much less than 50Ω.

In order to match impedances, it is necessary to transform the small capacitive load of the input transducer into a 50Ω resistive impedance, or as close to it as possible. This is a requirement both for any practical use of the device in a standard microwave circuit and even for testing of the device on commonly available microwave test equipment. Several different matching networks were developed for the correlators. A bulk component matching network was developed for quartz (figure 9). The bulk matching-element network is difficult to make broadband, so the resulting waveform exhibits undesirable distortion. Microstrip based impedance matching networks were also developed for both quartz and

lithium niobate correlators (figure 10). The microstrip approach proved to be simpler for matching to packaged devices due to the nature of the packaging parasitics. Using the microstrip matching approach, we tailored the length and number of finger-pairs of the correlator receiver section to give a total output impedance of approximately 50 Ω without any additional matching circuitry. The package inductance of about 3 nH and capacitance of about 1 pF contributed beneficially to matching the input IDT of the correlator. A single capacitor mounted to the microstrip board was used in conjunction with a 50 Ω microstrip trace to produce a broadband match with a final impedance close to 50 Ω at the center frequency of 2.45 or 2.70 GHz. SAW correlator insertion loss using these techniques was kept to about –14dB for a 31 chip correlator at 2.43 GHz with an 80 MHz bandwidth.
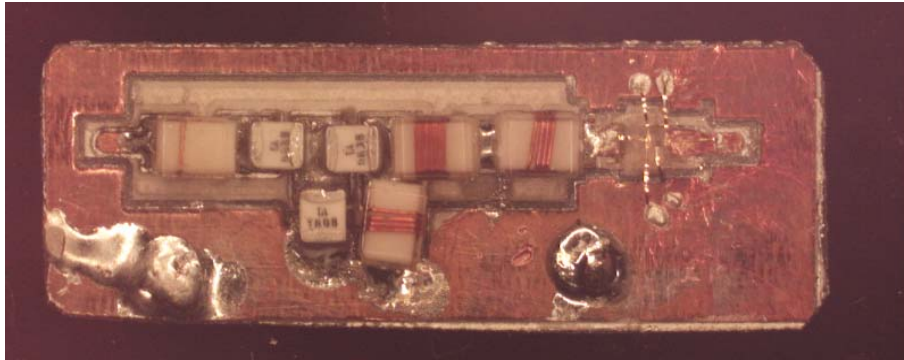

Figure 9: Quartz SAW correlator with bulk, broadband matching network.

Figure 10: SAW correlators mounted to microstrip headers with and without a package.

Temperature Effects and Material Choice

Temperature effects are important in communication-based applications. Drift of the SAW device center frequency is the primary temperature-induced effect. SAW correlator center frequency drift can have severe consequences, in spite of the wide input bandwidth that these devices possess. The effective bandwidth of a SAW correlator is determined in part by its chip bandwidth and is comparable to that of many SAW filters.

Frequency drift can be mitigated by selection of the substrate material type. ST-X quartz is a piezoelectric material suitable for surface wave propagation that has a zero temperature coefficient at room temperature. We fabricated a variety of devices on ST-X quartz and verified stable performance

over a temperature range of 7 to 100°C (figure 11). Unfortunately, ST-X quartz also has a low electromechanical coupling coefficient (0.16%). The electromechanical coupling coefficient determines the insertion loss of the SAW tag and therefore determines the useful range of the device. A low coupling coefficient in a correlator creates two significant problems. First, the resulting input IDT impedance can prove difficult in impedance matching. Second, the low insertion loss can render the useful operating range of the completed tag inadequate for the application.

The one-way insertion loss for an unmatched SAW frequency-type filter, useful for sensor-type tags, is about –25dB. A SAW filter was built at 2.45 GHz on quartz with 100 finger-pairs that are 90 λ long in both the input and the output IDTs. These devices have insertion losses that range from –25dB on down. This is a relatively poor value for filter applications, but the structure of a correlator will lead to even poorer insertion loss values.   The few-fingered input IDT of a correlator couples energy into a surface wave less efficiently than the many-fingered input of a typical SAW filter. An S-parameter measurement of a bi-phase modulated SAW correlator is not meaningful due to the phase reversals in the output IDT. However, an S-parameter measurement on a similarly sized SAW filter without any phase reversals in its output section will give a comparable estimate of the insertion loss of a correlator. Using this approach, an unmatched SAW filter built at 2.43 GHz on quartz with 2 finger-pairs (90 λ wide) in its input and 100 finger-pairs (90 λ wide) in its output has an insertion loss of –53 dB at the peak. This is the same physical structure that a 50-phase transition correlator at the same frequency has, and so this represents a measure of a correlator's insertion loss. It is a low enough value to render these quartz correlators unusable in most system applications. Attempts to improve coupling by using longer fingers failed due to lithographic alignment limitations.

These measurements on quartz establish the necessity of using a high coupling coefficient material such as lithium niobate in SAW correlator fabrication. Unfortunately, this limits the useful temperature range that such a communication device can be used over. The useful temperature range of a lithium niobate, SAW correlator-based communication device is determined by the length of the code, input bandwidth, and other correlator parameters. A useful rule of thumb is that a typical 31-chip correlator will respond adequately to an input frequency range of about 0.2% of its input center frequency. This corresponds to a temperature shift of only 20 °C in YZ-cut lithium niobate. Since the SAW correlator is a passive device, there is no self-heating, as in conventional powered electronics. Still, the useful temperature range is very limited, if the communication must be performed at a fixed frequency. It is important to note that communication can be frequency shifted to adjust to changes in ambient temperature. Such an approach is a straightforward solution for many applications.

There are reports in the literature of high coupling coefficient, zero-temperature coefficient thin films, such as AlN over sapphire [6]. These materials will completely alleviate the temperature drift problem. However, the technology to implement these films is not compatible with existing processing equipment in the laboratories used to make the SAWs, and so this technology was considered to be beyond the scope of this project. Future applications that require wide-temperature range SAW devices should develop this technology.
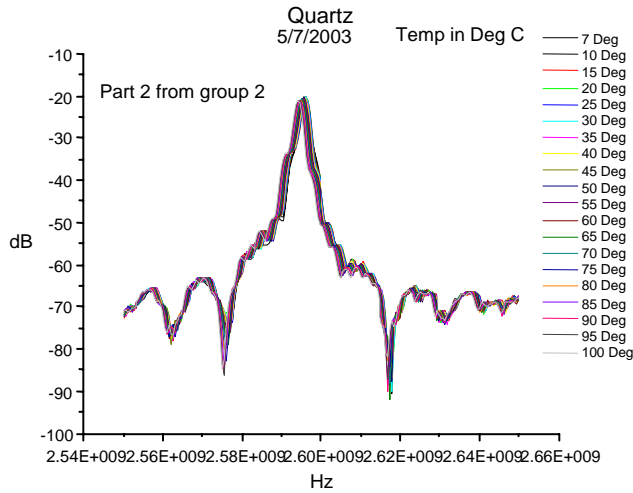
Figure 11: Quartz SAW S21 vs. frequency over temperature

Electrical Performance

The fixed correlators designed for 2.43 GHz ISM-band operation use codes of 30 cycles/chip to attain a bandwidth of about 80 MHz at the center frequency. UWB correlators with 4 cycles/chip in the same 2.43 GHz ISM band were also fabricated. An output signal from one of these UWB correlators is shown in figure 3. These correlators have output bandwidths of about 600 MHz, but otherwise have very similar performance to the 80 MHz wide devices. The PSL ratio for the UWB device shown in figure 3 is about 6:1. The output of an 80 MHz wide device is shown in figure 12. The PSL ratio for this typical device is also about 6:1. PSL ratios are greatly increased by the use of a properly designed square-law detector. The output PSL becomes about 25:1 at the detector output (figure 13). This is much more than adequate for the purposes of differentiation of a correct code from an orthogonal code, and that is the only reason to maintain a high PSL ratio in a radio based on these devices. For future work, significant improvements in overall PSL can most likely only be attained through optimization of the detector used to demodulate the output of the correlator.
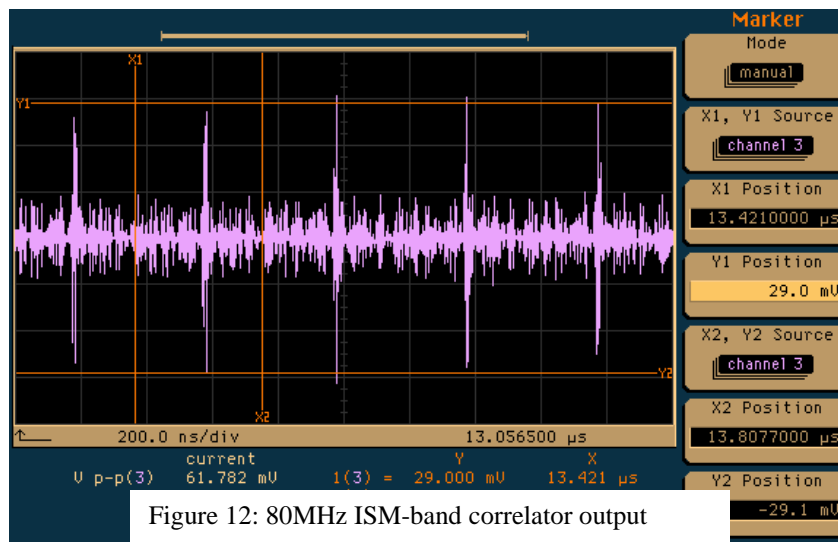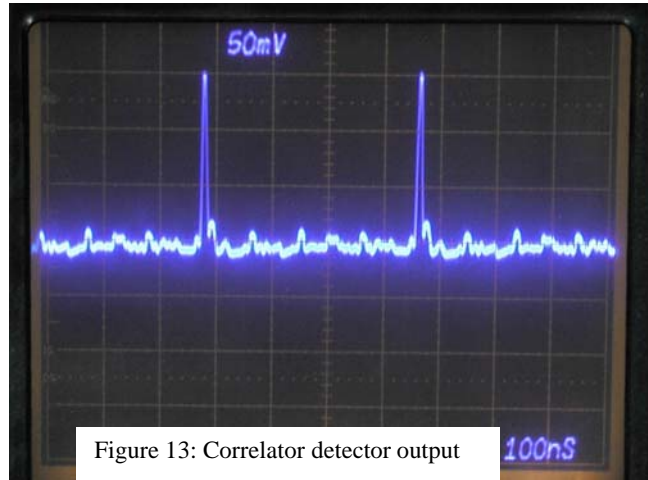

Figure 12: 80MHz ISM-band correlator output

19

Figure 13: Correlator detector output

PSAW Assembly
Version #1

Three different versions of the PSAW were designed, built, and tested. The first PSAW built was a fifteen-chip device fabricated from a lithium niobate correlator flip-chip bonded to a custom designed silicon switching array. The silicon base chip was fabricated in an American Microsystems, Inc. 0.5 μm CMOS process. The base IC contains the switches to configure the phases of each SAW chip. The SAW device itself was fabricated at the Compound Semiconductor Research Laboratory (CSRL) at Sandia National Laboratories. It was made on a lithium niobate substrate with electron beam lithography used to pattern the aluminum fingers and optical lithography used to pattern the electrical connections. The base IC and the top SAW device are joined together by flip-chip bump bonds using 50 x 50 μm pads lined up on the two chips. The combined hybrid device is shown in figure 14.
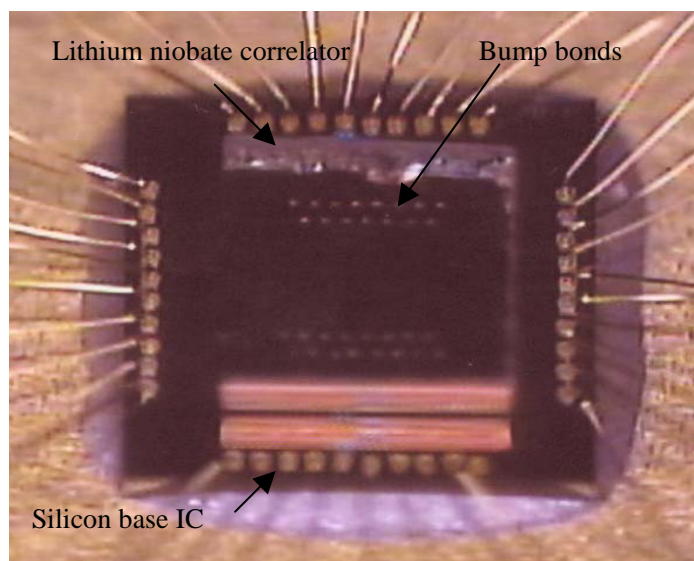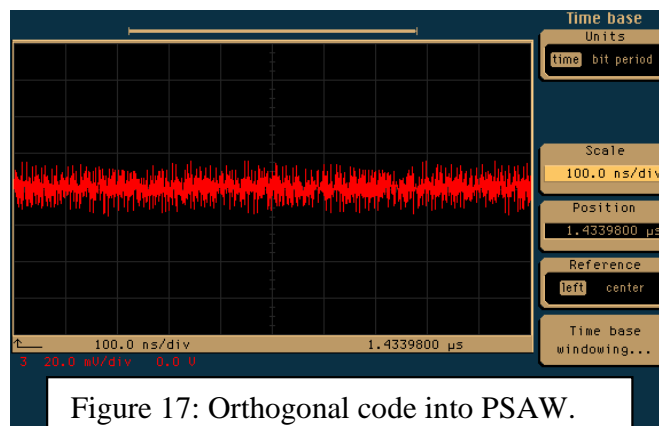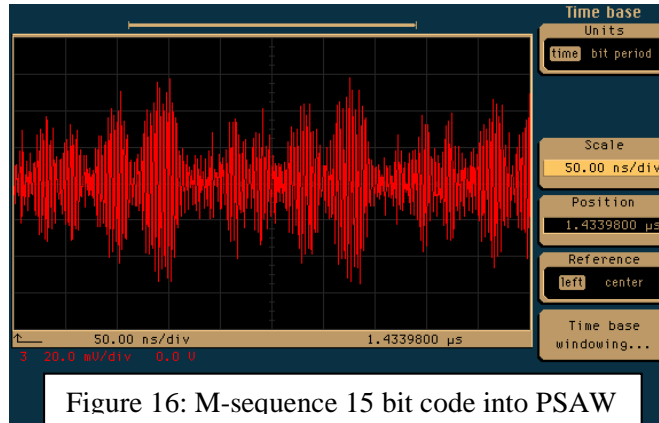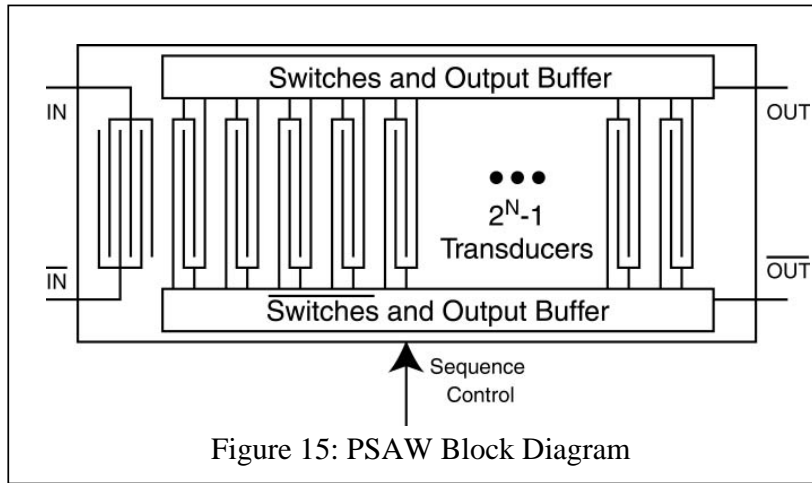

Figure 14: First PSAW, lithium niobate flip-chip bonded to Si switch array

Figure 15: PSAW Block Diagram

Figure 16: M-sequence 15 bit code into PSAW

Figure 17: Orthogonal code into PSAW.

A block diagram indicating the electrical connections is shown in figure 15. The diagram shows the electrical elements that are fabricated on both the silicon and lithium niobate substrates. The finger-pair structures shown in the center of the diagram are built on the piezoelectric lithium niobate substrate. The switches shown at the top and bottom of the diagram are built on the silicon substrate and connect to the finger-pair groups through the bump bonds that join the two chips.

Performance of the first version of the PSAW was found to be adequate to demonstrate the principle of programmability. The center frequency of the device, which is dependent on finger spacing, is not programmable and is set at 300 MHz. The output of the PSAW with a 15-code phase transition m-sequence code as an input is shown in fig. 16. The programming switches allow the phase reversal of any of the code phase groups. The correlation peaks are clear but overall PSL ratio is low. The output of the PSAW with an orthogonal code introduced into it is shown in fig. 17. This version of the PSAW exhibited good performance for a first device, but it was deemed important to produce a longer correlator.

Version #2
The second version of the PSAW was designed to build on the performance successes of the first version by increasing the operating frequency to 918 MHz and increasing the code length to 31chips. The design approach was similar to that used in the 300 MHz version of the PSAW. A lithium niobate correlator with a center frequency of 918 MHz was flip-chip bonded to a custom designed silicon switch array. The completed assembly is shown in figure 18. A completed chip in its custom test PCB is shown in figure 19. Because the device operates at high frequency, it needed to have a custom test fixture built.

The number of flip-chip bonds required to connect the two chips made the design physically difficult to build and mechanically unstable. A 31-chip correlator has at least 64 pads, and at 918 MHz, the correlator is over 2.8 mm long. Lithium niobate has a very different thermal coefficient of expansion than the underlying silicon base-IC. Additionally, inter-chip adhesive use is contra-indicated, as the SAW surface must be kept clear. As a result, even modest temperature changes of 50 ^{o}C stresses the part enough to cause disconnects in the flip-chip bonds. It was common for more than 75% of the assembled devices to fall apart before the packaging process was completed. Even after a device was successfully assembled and packaged, it was prone to developing internal disconnections or even falling apart. The resulting assembly was mechanically unreliable, though some valid data were collected on a few devices. The response to input codes on the devices that were tested exhibited a large signal output and a good PSL ratio, but the code response was very non-standard. The output did not respond as expected to normal PN codes, but responded significantly only to non-PN codes (i.e. codes with strong spectral characteristics). The output of one of the functioning devices to such a code is shown in figure 20. The conclusion drawn from the 918 MHz version of the PSAW is that flip-chip bonding is at this time an unreliable method of connecting two materials with highly dissimilar thermal coefficients of expansion. Unfortunately, this means that building programmable correlators with more than 15 chips at 918 MHz is not feasible given current packaging technology.
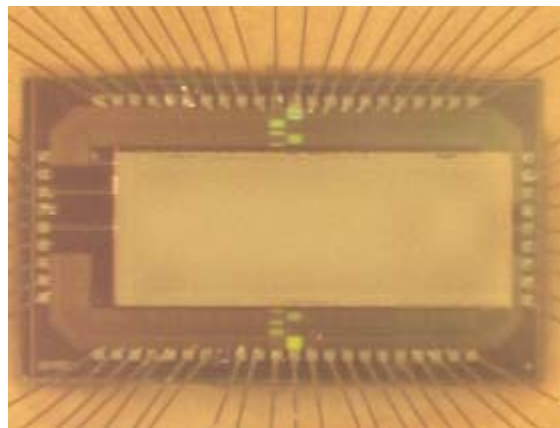

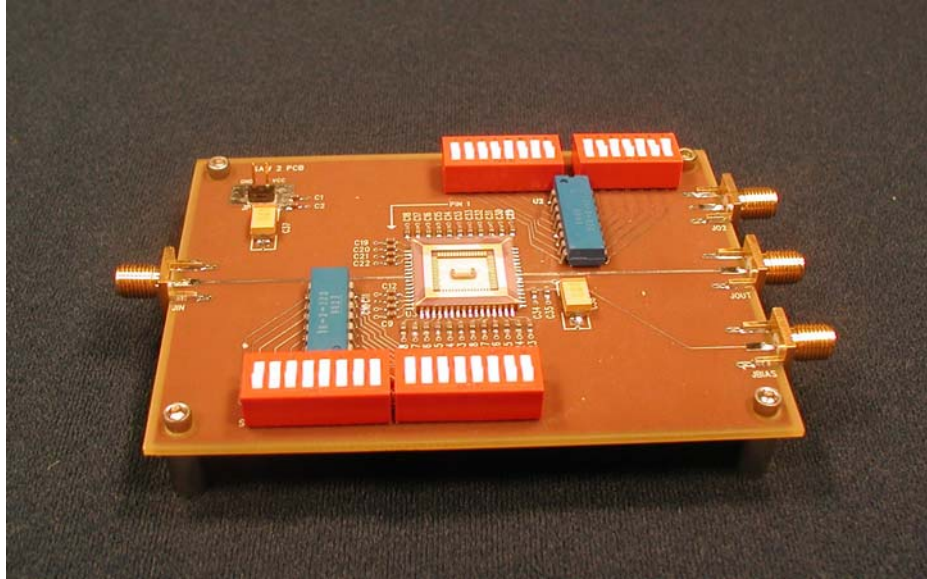Figure 18: 918 MHz PSAW flip-chip assembly.
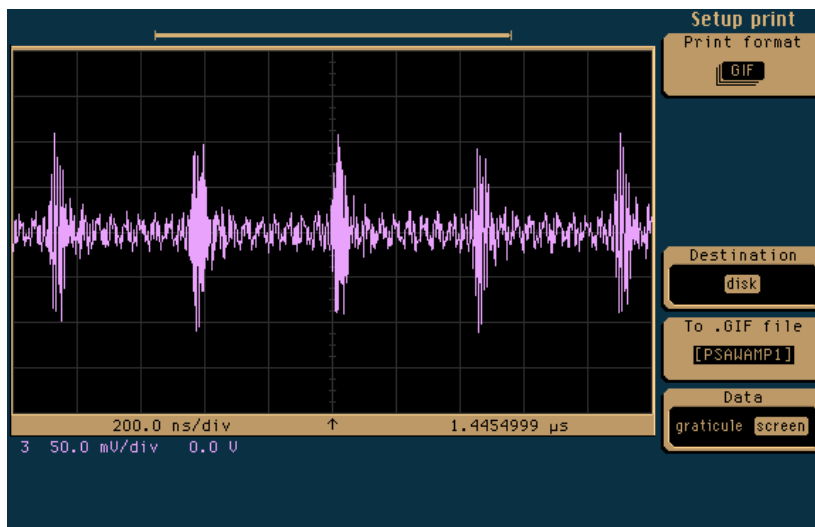
Figure 19: 918 MHz PSAW in its custom test PCB.

Figure 20: Output of 918MHz PSAW to non-PN code

Version #3
The third version of the PSAW was fabricated at 183 MHz (an IF sub-harmonic of 918 MHz) in order to avoid the flip chip bonding process problems encountered by working directly at the higher frequency. The assembly uses commercial multiplexer chips and a custom SAW correlator chip mounted on a conventional thick-film hybrid substrate using wire-bonds for electrical connections. The wire-bonds make reliable connections between the different temperature coefficient materials. The size of the complete PSAW assembly in its package is 1.25 x 1.25 x 0.125 inches. The substrate is an alumina base with three-layers of top-side fired gold alternating with two layers of fired insulator. The substrate is housed in a 44-pin gold plated Kovar package. Though size and parts count reductions are possible by integrating the individual devices into an ASIC, this is only cost effective for large production quantities.

Final PSAW Assembly Process

The version #3 PSAW uses conventional thick-film hybrid assembly methods. The alumina substrate was designed at Sandia and fabricated at Circuits Processing Technology, Oceanside, California. The PSAW units were then assembled at Sandia using the process shown in the following series of photos.

First steps:
- Attach Capacitors to the substrate with 8175 adhesive.
- Attach Mux die to the package with 8175 adhesive.
- Attach the inverters to the substrate with 8175 adhesive.
- Bake for 30 min at 150°C.
- Bond all Caps with Au Ball/Wedge or ribbon.
- Bond MUX around perimeter only with Al wire.
- Bond Inverters around perimeter only with Al wire.
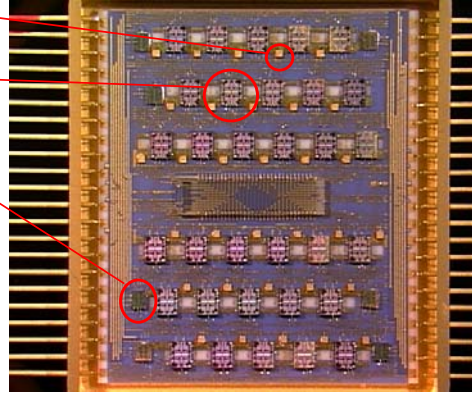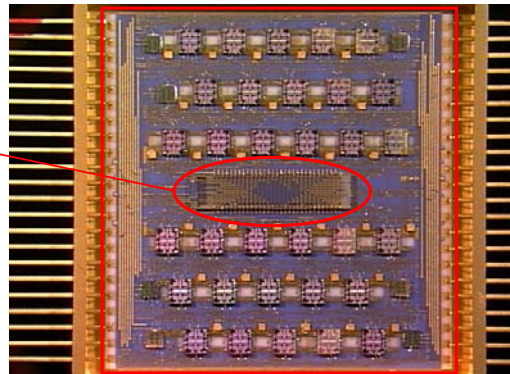

Second steps:

- Attach the substrate to the package with JM7000NC or conductive adhesive.
- Bake for 30 min at 150°C.
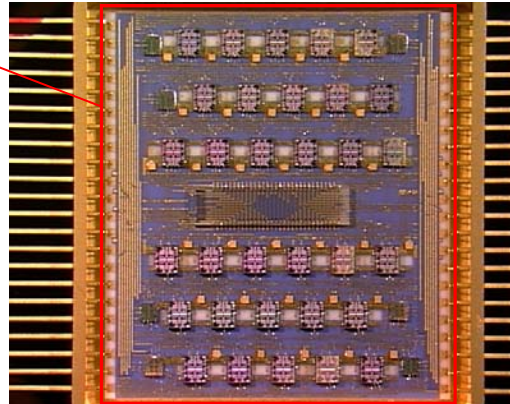
Third steps:
- Finish bonding MUX and Inverter die.
- Attach the SAW device to the substrate with JM7000NC-one drop at left, center, and right to prevent oozing onto neighboring bond pads.
- Bake for 30 min at 150°C.
- Bond the SAW device with Au ball or ribbon.

Fourth steps:

- Wire bond substrate to package pins with Au ribbon.
- Tape lid onto package.
- Burn-in and test the part.
- Attach lid onto package with room temperature curing silver epoxy (TRA-DUCT by Tra-Con Inc.).
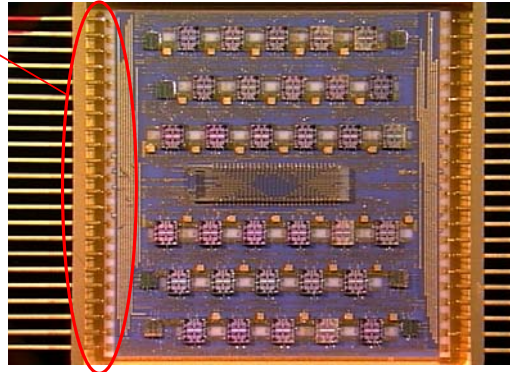
PSAW Performance
The third version of the PSAW satisfies the multiple requirements of adequate ruggedness, low power consumption, good signal-to-noise ratio, good PSL ratio, and small size. The use of wire-bonds and proven hybrid assembly techniques makes for a device that easily withstands storage temperatures of –55 to +150 ^{o}C. Power consumption is typically about 10mW at 5v, the design voltage. For some units power consumption is less than 5mW at 5v. The PSAW operates well at voltages much below the design voltage, and power consumption is commensurately lower. Typical power consumption drops to about 3mW at 4v. The PSAW operates on as little as 1.5v with very little signal degradation. At 1.5v, the PSAW consumes about 375µW. Overall signal level decreases to about 40% of that seen at the design voltage, but the PSL ratio exhibits very little degradation. The power consumption of the PSAW is very low and represents a small fraction of the operating power required by the other radio components in any communication system.

A wide-ranging study of different 31-chip m-sequence codes introduced with different code start locations was performed on the PSAW. The results indicate that the PSAW is quite usable in systems employing a small number of receiver/transmitters. The purpose of the study was to determine whether there is sufficient POP (or PSL) ratio in the PSAW to adequately differentiate a desired from an undesired code. This is the entire purpose of the POP ratio: to differentiate received codes into correct and orthogonal codes. That is, if the received code is the code programmed into the PSAW, then it must have a higher POP ratio than an orthogonal code received into the PSAW with the same program settings. The test results conclusively indicate that POP ratio in the PSAW is adequate for differentiation of a set of orthogonal 31-chip codes, as the subsequent analysis will indicate.

The study of different codes centers uses the 6 different maximal, or m-sequence, codes available for a 31-chip sequence. These codes are listed as follows:

1) Code A: 1111100011011101010000100101100
2) Code B: 1111101110001010110100001100100
3) Code C: 1111101000100101011000011100110
4) Code X: 1111100100110000101101010001110
5) Code Y: 1111101100111000011010100100010
6) Code Z: 1111100110100100001010111011000

These codes were tested in the PSAW by transmitting from a bit error rate tester (BERT), the Microwave Logic GigaBERT 1400, with the digitally coded signal at twice the center frequency of the correlator.

The receiver section of the PSAW was programmed with either a matching code or an orthogonal code and the results were recorded. The output of the PSAW was filtered through a 200MHz lowpass filter and the results were recorded on a Tektronix TDS3054 oscilloscope in an Excel compatible format. It is important to note that the receiver will respond with a correlation peak if it is programmed to any sequential permutation of the correct code listed above. That is, the PSAW can be programmed with one of the codes listed above with the code starting at any place in the sequence. Mathematically, all of these permutations should respond equally. In actuality, different permutations give better or worse performance, depending on second order physical effects within the correlator itself. These codes were tested under a wide range of different permutations.

It is helpful to consider some of the data from various correlator responses. In figure 21, code X is transmitted from the BERT into the PSAW programmed to respond to code X starting at chip position 1 in the listing shown above. The data recognition problem on such a signal consists of differentiating the correlation peaks from the side lobe signals. This can be accomplished with a trivial algorithm consisting of a level detecting comparator set at 4 times the RMS signal level. This will set a trip-line at about 10mV for the signal level shown. Any signal above this level represents a data bit, any signal below this level represents noise, or not a data bit. The exact threshold can be set at something more or less than 4 times the long-time filtered RMS level, depending on the desired bit error rate. For the signal shown in figure 21, a threshold level set at slightly below 10mV will give a bit error rate of less than 10^{-5} per sample, a low value for raw data.
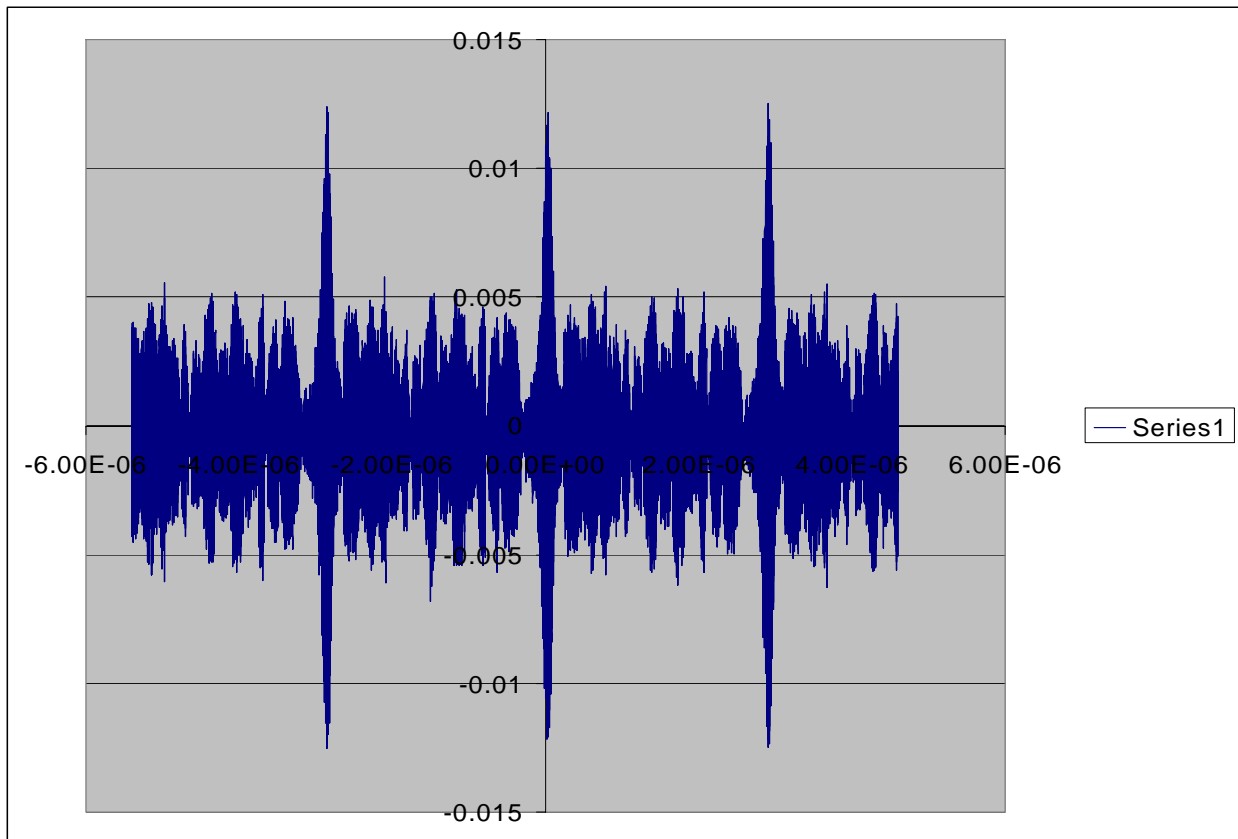

Figure 21: PSAW output with code X sent to correlator programmed for code X.

In figure 22, code Z is transmitted from the BERT to the PSAW programmed to respond to code X starting at the first chip position. Here the two codes are orthogonal, and the PSAW should respond with

no correlation peak. The overall RMS level does increase, due to an increase in energy in the sidelobes. Applying the same algorithm as used for the previous example entails setting a detection threshold at 4 times the RMS level. Because the RMS level is somewhat higher for the orthogonal code, this will put the threshold at about 12mV. A 12mV detection threshold is well above the apparent signal level, and the false detection rate is again below 10^{-5} per bit.
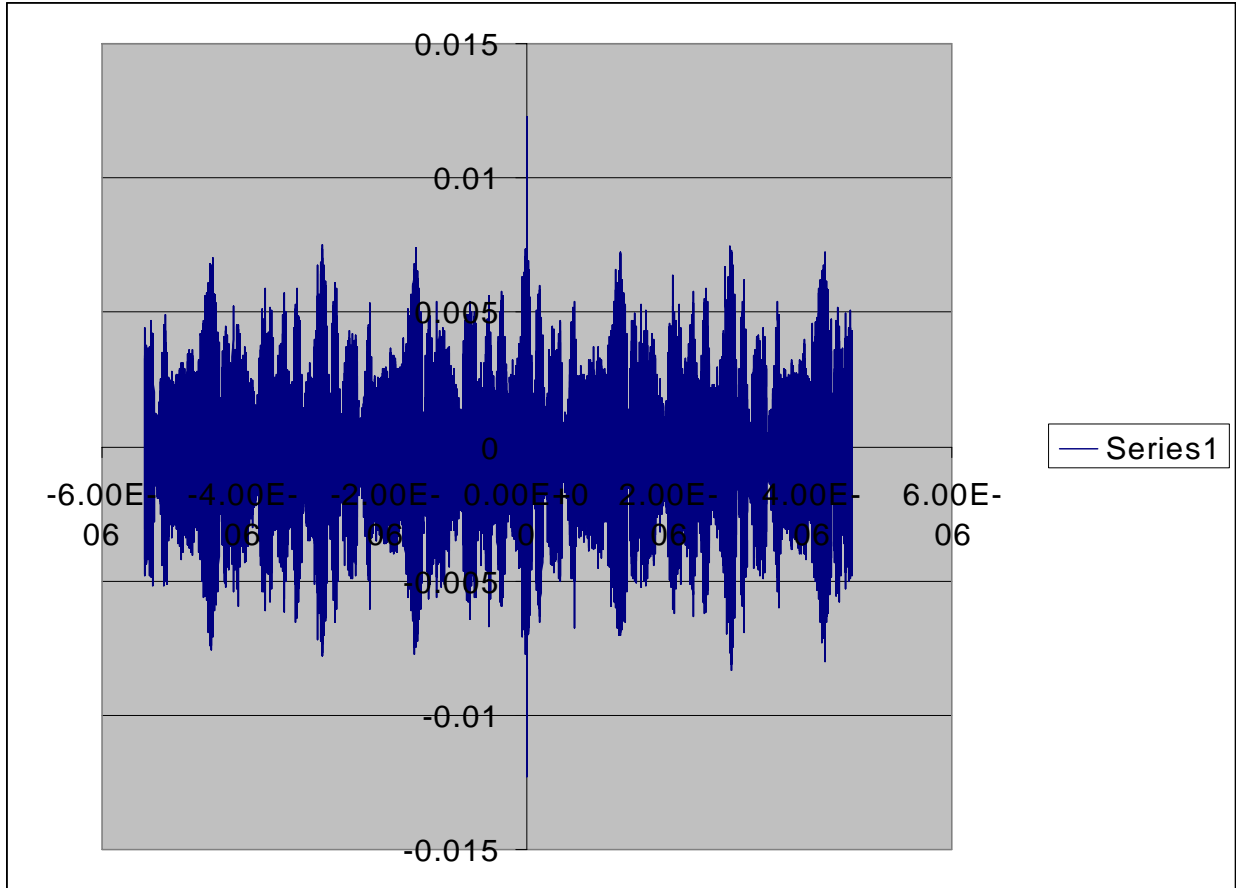

Figure 22: PSAW with code Z sent to correlator programmed for code X.

In figure 23, code X is transmitted from the BERT in exactly the same manner as for figure 21, except that the PSAW is programmed to receive code X starting at chip 12. Mathematically there is no change to the signal or the expected response, but the output signal exhibits a noticeable decrease in sideband energy observable as a decrease in RMS signal level. Also, the correlation peak voltage is slightly higher than the peaks in figure 21. This represents a small improvement in signal quality. Each shift in starting location for the code programmed into the PSAW will give a small change in the appearance of the output signal. This occurs with no change to either the code transmitted or the code received. Depending on the nature of the detection algorithm, one particular permutation may have a significant advantage over another. We observed and documented a large number of different receiver code permutations with the PSAW.

In figure 24, code X is transmitted from the BERT in exactly the same manner as was done for figures 21 and 23. Code X is also programmed into the PSAW receiver but with a shift to the right of 27 chips. The output signal in this figure shows significant degradation from the signal in either figure 21 or figure 23. The sidelobe energy has increased at the expense of the peak signal. Using the PSAW with this permutation of code X will give a decreased detection range between orthogonal codes and is undesirable.

This result signifies the importance of permuting the codes that will be used with the PSAW to find the permutations that are optimal for the code differentiation algorithm being used.
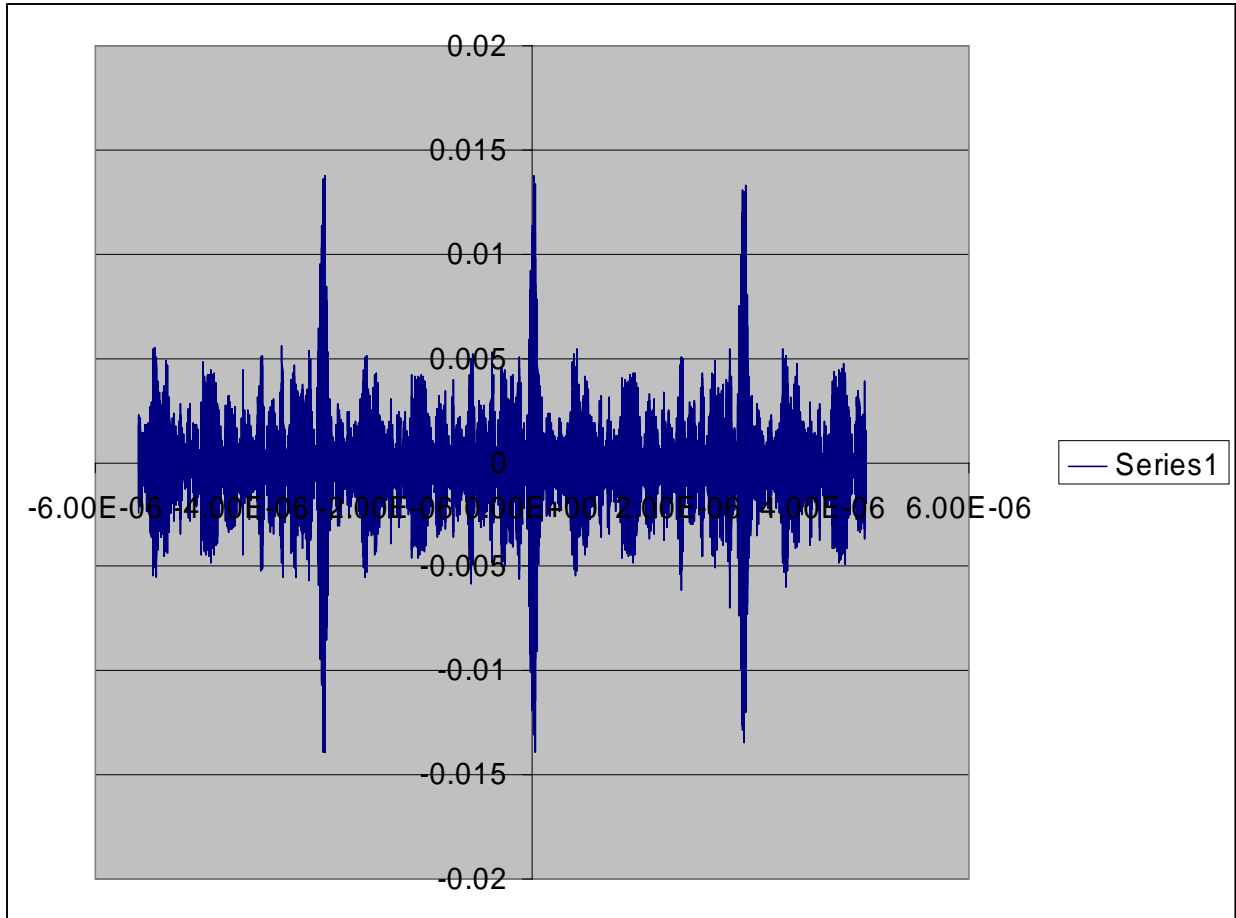

Figure 23: PSAW output receiving code X programmed for code X shifted 12 chips right.
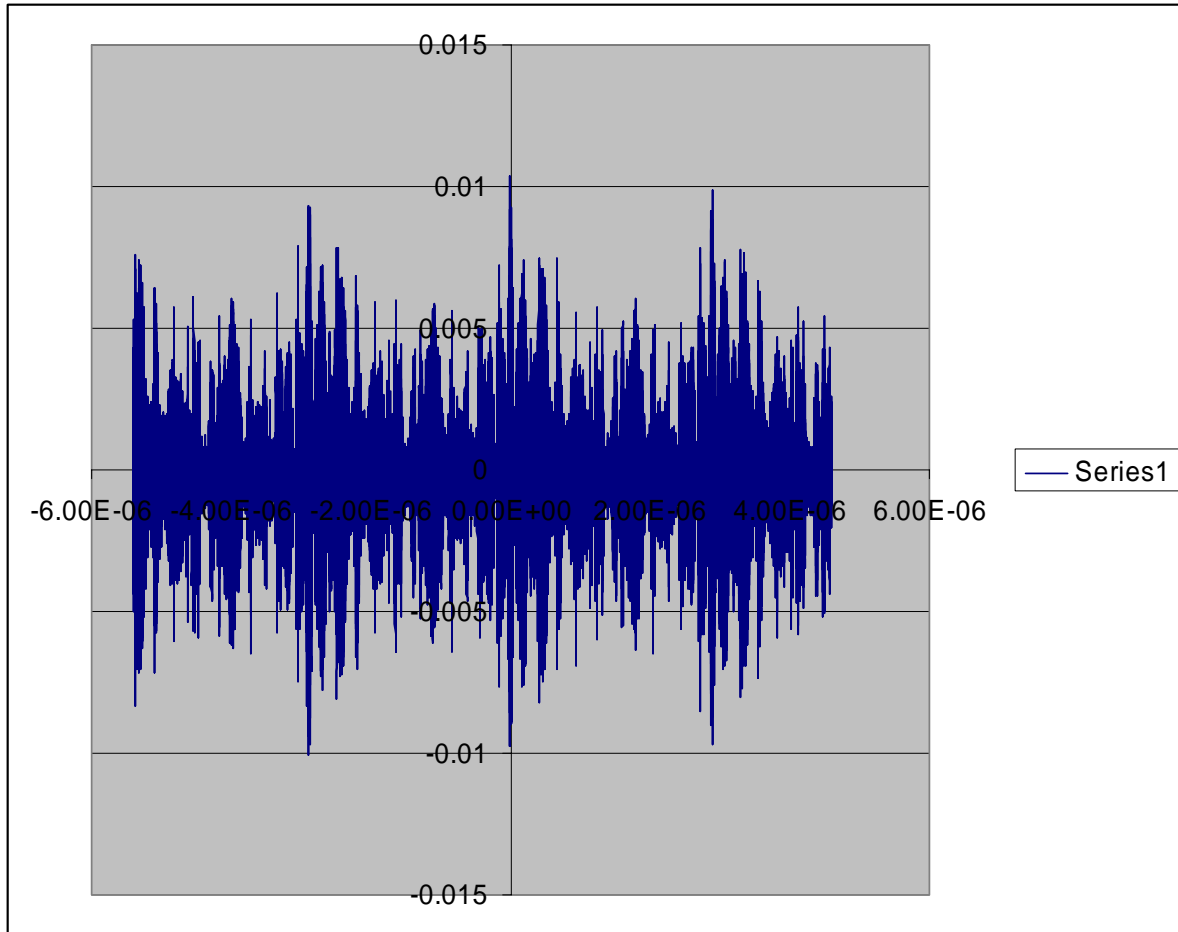
Figure 24: PSAW output receiving code X programmed for code X shifted 27 chips right.

Conclusion

A number of different fixed and programmable SAW correlators were developed and tested for the NASA/ Sandia Low-Power Communication System Project. It was demonstrated that good performance in terms of size, power consumption, signal-to-noise ratio, and POP ratio were obtained with the final versions of these components. It was shown that the use of the SAW correlator enables the elimination of large portions of signal processing electronics in radio design.   This is accomplished by performing high speed, sophisticated signal processing passively using the SAW IDT. The possibilities are excellent for using these components to build very small, low-parts count, very low power radios.

References

1) Hagon, P.J. and Wheatley, C.E., "Programmable Analog Matched Filters," *Microwave Journal,* July 1974, pp. 42-45.
2) Freret, P., et al, "Applications of Spread-Spectrum Radio to Wireless Terminal Communications," *Proc. NTC 80,* vol. 4 (1980), pp. 69.7.1-69.7.4.
3) Eschenbach, R., "Applications of Spread Spectrum Radio to Indoor Data Communications," *MILCOM '82 IEEE Military Comm. Conf.,* vol. 2 (1982), pp. 34.5-1 –34.5-3.
4) Brocato, R.W., et al, "High Frequency SAW Correlator Module," *Proc. 53rd IEEE Elec. Comp. and Tech. Conf.,* May 2003, pp. 458-463.
5) Brocato, R.W., et al, "UWB Communication Using SAW Correlators," *Proc. 2004 IEEE Radio and Wireless Conf.,* Sept. 2004, pp. 267-270.
6) Nakase, H., et al, "One Chip Demodulator Using RF Front-End SAW Correlator for 2.4GHz Asynchronous Spread Spectrum Modem," *IEEE Proc. of Wireless Networks, Catching the Mobile Future,* Sept. 1994, pp.374-378.
7) Kuhne, J., et al, "A Demonstrator for a Low-Cost, Cordless, Multi-Carrier Spread-Spectrum System," *IEEE Trans. On Ultrasonics, Ferroelec., and Freq. Control,* vol. 47, no. 1, Jan. 2000, pp. 58-64.
8) Hachigo, A., et al, "10GHz Narrow Band SAW Filters using Diamond," *Proc. 1999 IEEE Ultrasonics Symposium*, pp. 325-328.
9) Campbell, C.K., *Surface Acoustic Wave Devices for Mobile and Wireless Communications,* Academic Press, 1998, p. 11.
10) Biran, A., "Low-Sidelobe SAW Barker 13 Correlator," *IEEE 1985 Ultrasonics Symp.,* pp. 149-152.
11) Ruppel, C.W., et al, "Review of models for low-loss filter design and application," *Proc. 1994 IEEE Ultrasonics Symposium,* vol. 1, 1994, pp. 313-324.

Appendix: Layout Files

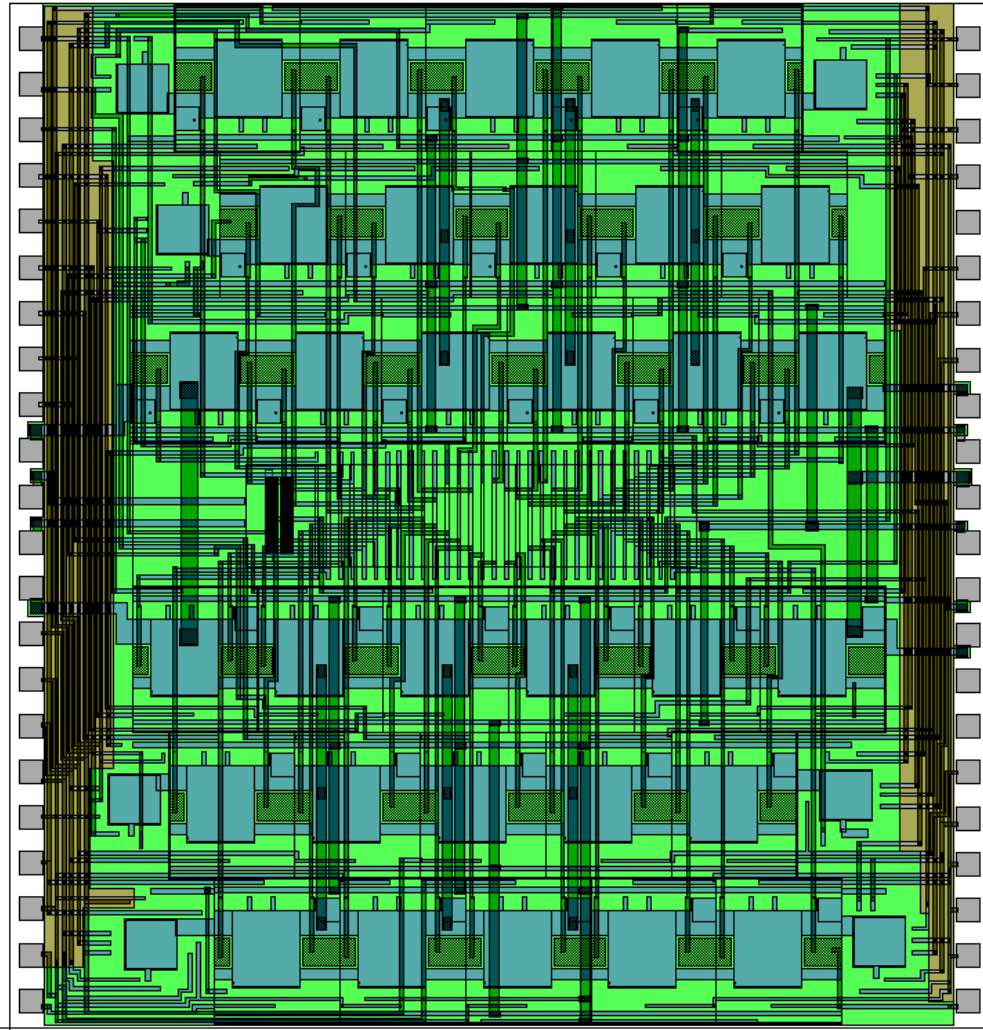**Figure 25: PSAW 3- layer metal on alumina substrate layout**

Dimensions: 1.10 x 1.05 inches

17 finger-pair
Driver IDT

31 chip receiver IDT with 17 finger/pairs per chip
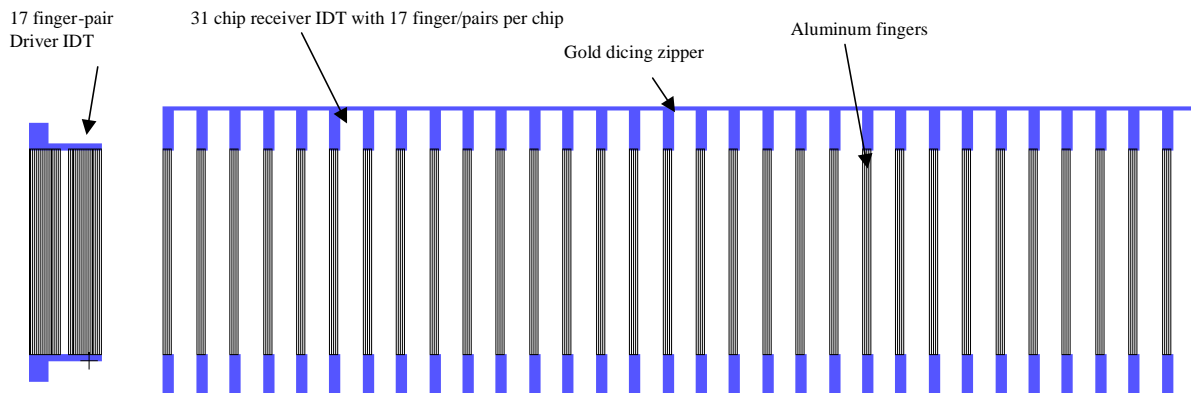
Gold dicing zipper

Aluminum fingers

Figure 26: PSAW layout with metal zipper for testing

* SPICE NETLIST for 15-chip correlator simulation
*
* Correlator Simulation Testbench   Revised: March 20, 2002
* CORRTEST.SCH   Revision:
* R.W. Brocato
*
*
*
*
S1 VIN_0 10015 DATA1_0 0 RELAY2
S2 VIN_0 10016 DATA0_0 0 RELAY2
VCC1 VCC_0 0 PWL(0PS 0V 100PS 1V)
U_DSTM1 STIM(1,0) VCC_0 0 DATA1_0 IO_STM STIMULUS=D1
U_DSTM2 STIM(1,0) VCC_0 0 DATA0_0 IO_STM STIMULUS=D2
IOUT VOUT_0 0 DC 0
VINPHASE 10015 0 SIN(0V 1V 2.5GHZ 100PS 0 0)
VOUTPHASE 10016 0 SIN(0V 1V 2.5GHZ 100PS 0 180)
XCOR1 0 VOUT_0 VIN_0 0 COR15C
.SUBCKT COR15C SIG0 SIG1 VIN VSSIN
XDRIVER VIN AC_DRV1_0 VSSIN AC_DRV0_0 DRIVE2P
XDELAY1 AC_DRV1_0 AC_REC1_0 AC_DRV0_0 AC_REC0_0 DELAY1
XRECEIVER AC_REC0_0 SIG0 AC_REC1_0 SIG1 REC15C
.ENDS
.SUBCKT DRIVE2P DRVIN DRVOUT DRVSSIN DRVSSOUT
RIN DRVIN 10028 50
CIN 10028 DRVSSIN 0.15PF
TENDZON1 10033 0 10030 0 Z0=179.5K F=2.5GHZ NL=10
REND1 10033 0 60K
XD1 10035 10031 DRVSSIN DRVIN 0 10030 FINGER1
XD2 DRVSSOUT DRVOUT DRVSSIN DRVIN 10035 10031 FINGER1
.ENDS
.SUBCKT FINGER1 DRVO0 DRVO1 IN0 IN1 REFL0 REFL1
RDUM1 VDRV1_0 10050 50
REST REFL0 DRVO0 1
RDZ1 10052 VDRV1_0 180K
RDZ2 VDRV1_0 10053 180K
RDZ3 10054 VDRV0_0 180K
RDZ4 VDRV0_0 10055 180K
E1 10050 VDRV0_0 IN1 IN0 0.1
TMETALP1 REFL1 REFL0 10052 REFL0 Z0=168K F=2.5GHZ NL=0.06322
TMETALP2 10052 REFL0 10058 REFL0 Z0=168K F=2.5GHZ NL=0.06322
TMETALP3 10059 REFL0 10053 REFL0 Z0=168K F=2.5GHZ NL=0.06322
TMETALP4 10053 REFL0 10060 REFL0 Z0=168K F=2.5GHZ NL=0.06322
TMETALN1 10061 REFL0 10054 REFL0 Z0=168K F=2.5GHZ NL=0.06322
TMETALN2 10054 REFL0 10062 REFL0 Z0=168K F=2.5GHZ NL=0.06322
TMETALN3 10063 REFL0 10055 REFL0 Z0=168K F=2.5GHZ NL=0.06322
TMETALN4 10055 REFL0 10064 REFL0 Z0=168K F=2.5GHZ NL=0.06322
TSPACE1 10058 REFL0 10059 REFL0 Z0=179.5K F=2.5GHZ NL=0.12356
TSPACE2 10060 REFL0 10061 REFL0 Z0=179.5K F=2.5GHZ NL=0.12356
TSPACE3 10062 REFL0 10063 REFL0 Z0=179.5K F=2.5GHZ NL=0.12356
TSPACE4 10064 REFL0 DRVO1 REFL0 Z0=179.5K F=2.5GHZ NL=0.12356

.ENDS
.SUBCKT DELAY1 DELIN DELOUT DVSSIN DVSSOUT
REST2 DVSSIN DVSSOUT 1
TLINE2 DELIN DVSSIN DELOUT DVSSIN Z0=179.5K F=2.5GHZ NL=5
.ENDS
.SUBCKT REC15C RCVSSIN RCVSSOUT RECIN RECOUT
COUT RECOUT RCVSSOUT 0.3PF
ROUT RECOUT RCVSSOUT 50
RCHP1 RECOUT 10102 0.2
RCHP2 RECOUT 10103 0.2
RCHP3 RECOUT 10104 0.2
RCHP4 RECOUT 10105 0.2
RCHP5 RECOUT 10106 0.2
RCHP6 RECOUT 10107 0.2
RCHP7 RECOUT 10108 0.2
RCHP8 RECOUT 10109 0.2
RCHP9 RECOUT 10110 0.2
RCHP10 RECOUT 10111 0.2
RCHP11 RECOUT 10112 0.2
RCHP12 RECOUT 10113 0.2
RCHP13 RECOUT 10114 0.2
RCHP14 RECOUT 10115 0.2
RCHP15 RECOUT 10116 0.2
TENDZON2 10133 0 10134 0 Z0=179.5K F=2.5GHZ NL=10
REND2 10134 0 60K
XCHIP1 10102 RCVSSOUT RCVSSIN RECIN 10136 10119 CHIP1_8
XCHIP2 10103 RCVSSOUT 10136 10119 10137 10120 CHIP1_8
XCHIP3 RCVSSOUT 10104 10137 10120 10138 10121 CHIP1_8
XCHIP4 RCVSSOUT 10105 10138 10121 10139 10122 CHIP1_8
XCHIP5 10106 RCVSSOUT 10139 10122 10140 10123 CHIP1_8
XCHIP6 RCVSSOUT 10107 10140 10123 10141 10124 CHIP1_8
XCHIP7 10108 RCVSSOUT 10141 10124 10142 10125 CHIP1_8
XCHIP8 RCVSSOUT 10109 10142 10125 10143 10126 CHIP1_8
XCHIP9 RCVSSOUT 10110 10143 10126 10144 10127 CHIP1_8
XCHIP10 RCVSSOUT 10111 10144 10127 10145 10128 CHIP1_8
XCHIP11 RCVSSOUT 10112 10145 10128 10146 10129 CHIP1_8
XCHIP12 10113 RCVSSOUT 10146 10129 10147 10130 CHIP1_8
XCHIP13 10114 RCVSSOUT 10147 10130 10148 10131 CHIP1_8
XCHIP14 10115 RCVSSOUT 10148 10131 10149 10132 CHIP1_8
XCHIP15 RCVSSOUT 10116 10149 10132 0 10133 CHIP1_8
.ENDS
.SUBCKT CHIP1_8 IOUT0 IOUT1 WAVI0 WAVI1 WAVO0 WAVO1
TGAP1_MTL WAVI1 WAVI0 10112 WAVI0 Z0=168K F=2.5GHZ NL=3.54029
TGAP1_SPC 10112 WAVI0 10113 WAVI0 Z0=179.5K F=2.5GHZ NL=3.45971
XD8 IOUT0 IOUT1 WAVO0 WAVO1 WAVI0 10113 FPOUT
.ENDS
.SUBCKT FPOUT IO0 IO1 OUT0 OUT1 REFL0 REFL1
GFP1 IO1 IO0 VREC1_0 VREC0_0 0.01
REST3 REFL0 OUT0 1
RZX1 10132 VREC1_0 100MEG
RZX3 10134 VREC0_0 100MEG

```
RZX4 VREC0_0 10135 100MEG
RZX2 VREC1_0 10133 100MEG
TMTLP1 REFL1 REFL0 10132 REFL0 Z0=168K F=2.5GHZ NL=0.06322
TMTLP2 10132 REFL0 10138 REFL0 Z0=168K F=2.5GHZ NL=0.06322
TMTLP3 10139 REFL0 10133 REFL0 Z0=168K F=2.5GHZ NL=0.06322
TMTLP4 10133 REFL0 10140 REFL0 Z0=168K F=2.5GHZ NL=0.06322
TMTLN1 10141 REFL0 10134 REFL0 Z0=168K F=2.5GHZ NL=0.06322
TMTLN2 10134 REFL0 10142 REFL0 Z0=168K F=2.5GHZ NL=0.06322
TMTLN3 10143 REFL0 10135 REFL0 Z0=168K F=2.5GHZ NL=0.06322
TMTLN4 10135 REFL0 10144 REFL0 Z0=168K F=2.5GHZ NL=0.06322
TSPC1 10138 REFL0 10139 REFL0 Z0=179.5K F=2.5GHZ NL=0.12356
TSPC2 10140 REFL0 10141 REFL0 Z0=179.5K F=2.5GHZ NL=0.12356
TSPC3 10142 REFL0 10143 REFL0 Z0=179.5K F=2.5GHZ NL=0.12356
TSPC4 10144 REFL0 OUT1 REFL0 Z0=179.5K F=2.5GHZ NL=0.12356
.ENDS
.END
```

Distribution

8	MS0874	Robert W. Brocato, 1751
4	MS0874	David W. Palmer, 1751
1	MS0874	Glenn D. Omdahl, 1751
1	MS0874	Gregg A. Wouters, 1751
1	MS0874	Matthew A. Montano, 1751
1	MS0874	Emmett J. Gurule, 1751
1	MS0874	Christopher L. Gibson, 1751
1	MS0603	Joel R. Wendt, 1743
1	MS0603	Jonathan D. Blaich, 1763
1	MS0874	Vincent M. Hietala, 1738
1	MS0865	Regan W. Stinnett, 1903
1	MS1371	Dianna S. Blair, 6926
1	MS1071	Michael G. Knoll, 1730
1	MS1202	John P. Anthes, 5940
1	MS0529	Michael B. Murphy, 2346
1	MS0529	Kenneth W. Plummer, 2346
1	MS0986	Judd A. Rohwer, 2664
1	MS0782	Rebecca Darnell Horton, 4148
1	MS1078	Stephen J. Martin, 1707
1	MS0123	LDRD Office, Donna L. Chavez
1	MS9018	Central Technical Files, 8945-1
2	MS0899	Technical Library, 9616